physica status solidi b

phys. stat. sol. (b) **243**, No. 9, 2164–2169 (2006) / **DOI** 10.1002/pssb.200666815

Electronic structure of Pd-covered (10,0) carbon nanotube

Wenguang Zhu and **Efthimios Kaxiras***

Department of Physics and Division of Engineering and Applied Sciences, Harvard University, Cambridge, MA 02138, USA

Received 12 April 2006, accepted 1 May 2006
Published online 10 July 2006

PACS 71.15.Mb, 73.20.–r, 73.22.–f, 73.40.Ns

We report a first-principles study on the electronic structure of a semiconducting (10,0) single-wall carbon nanotube fully covered by Pd electrode, which closely resembles experimental setups. The equilibrium structure, charge transfer effects, electrostatic potentials, and the density of states are studied in detail, in order to establish whether a barrier exists or not between the natotube and the metal contact.

1 Introduction

Since IIjima's discovery of carbon nantotubes (CNTs) [1], these important one-dimensional systems have received extensive attention as promising building blocks for future nanoelectronics because of their small size, reliable structural strength and extraordinary electronic properties [2, 3]. Recent studies [4–9] have demonstrated that an individual semiconducting nanotube can either operate as conventional MOSFET [10] or an unconventional Schottky barrier transistor [11] when it forms a contact with a metal electrode. The interaction between the carbon nanotube and the metal contacts and the resulting electronic structure effects are crucial for the performance of the carbon nanotube field-effect transistor (CNFET) [11, 12]. Experimental studies showed that the metal used as electrode and the variation in nanotube diameter are the two main features responsible for the performance of CNFET [13], with the best performance achieved by combining Pd contacts with CNTs of diameter larger than 1.4 nm. In these experimental studies, the details of the interface geometry are believed to affect the nature of the contact. Theoretically, several model systems have been used to address certain aspects of the structure and electronic properties of the metal/semiconducting CNT contacts [14–16], such as the Schottky barrier, tunneling barrier and charge transfer effect, in which the metal/CNT contacts are modeled by simply having the nanotubes adsorbed on flat metal surfaces or placing them between two parallel metal surfaces. There is, however, a need to describe the metal/CNT contact in more realistic geometries, in order to establish the dependence of these properties on the model.

In this paper, we use first-principles calculations to study the electronic structure of the contact between semiconducting (10,0) single-wall carbon nanotube (SWCNT) and Pd metal electrode in a fully covered geometry that resembles closely the experimental setups [13]. We find that the surrounding metal electrode induces a deformation on the nanotube when the combined structure is fully optimized. The calculated electrostatic potential reveals that, in the channels relevant to electron transport, there are no barriers at the interface of the nanotubes and the metal electrode. Charge difference analysis shows that electrons are transferred from the nanotube as well as from the metal Pd electrode to the interface region. Finally, the electronic density of states reveals that the deformation and interface states induced

* Corresponding author: e-mail: kaxiras@physics.harvard.edu

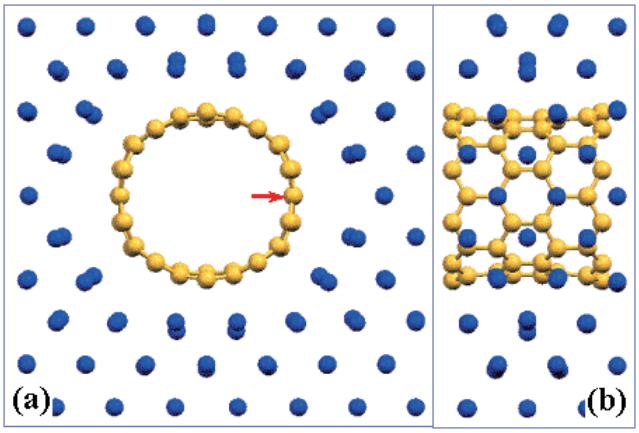

Fig. 1 (online colour at: www.pss-b.com) Atomic structure of the Pd/(10,0) CNT system, including full relaxation: Two views of the (10,0) nanotube fully covered by Pd are shown, (a) along, and (b) perpendicular to the nanotube axis. The red arrow in (a) indicates the C atom we chose as a reference for lining up the energy levels in the density of states plots (Fig. 4).

by the Pd electrode introduce electronic states in the region of the gap of the semiconducting (10,0) SWCNT.

Our first-principles calculations are based on density functional theory and the Perdew–Wang 1991 version of the generalized gradient approximation (PW91-GGA) [17], as implemented in VASP [18]. Default plane-wave cut-offs from the GGA ultrasoft-pseudopotential database [19] are used for both Pd and C in the calculations. The Monkhorst–Pack scheme [20] is employed for Brillouin Zone sampling. Optimized atomic geometries are achieved when the magnitude of the forces on all unconstrained atoms is smaller than 0.03 eV/Å. These choices of computational parameters produce a lattice constant of 3.962 Å for bulk fcc Pd, compared to the experimental value of 3.890 Å; the calculated diameter of the free standing (10,0) SWCNT is 7.90 Å.

Here, we use a perfect Pd fcc crystal and remove just enough Pd atoms for the nanotube to fit into the opening to model an infinite (10,0) carbon nanotube fully covered by the Pd electrode. The constructed supercell is shown in Fig. 1. The direction of the nanotube axis is parallel to the ⟨110⟩ direction of the Pd crystal. In this direction, three periods of the Pd crystal (2.80 Å × 3) match very well with two periods of the zigzag (10,0) nanotube (4.26 Å × 2), with a difference in lattice parameter between the two superstructures of only 1.4%. The size of the holes in the metal is chosen as small as possible to accommodate the nanotube, the only requirement being that the combined system have a net energy gain relative to the isolated components. This requirement ensures that the model contact does not involve unphysical configurations with atoms that are too close. The cross section of the holes in the Pd lead is hexagonal, with the inner surfaces consisting of the close-packed Pd (111) and (100) facets. Figure 1 shows the optimized structures, in which the (10,0) SWCNT is deformed in the radial direction. The shortest distances between C and Pd atoms are 2.22 Å.

The calculated self-consistent-field electrostatic potential of the Pd covered (10,0) SWNT is presented in Fig. 2. Figure 2(a) and (b) are constant-value contours of the electrostatic potential on planes perpendicular to the nanotube axis, indicated by the red lines shown in the insets. Blue and red areas in these contour plots represent regions where the electrostatic potential is lower and higher the Fermi level of the system, respectively. The other two representative contour plots of electrostatic potential, shown in Fig. 2(c) and (d), correspond to cross sections passing through the planes on which the carbon atoms of the nanotube are in the closest contact with surrounding Pd atoms; these cross sections are indicated in the inset of Fig. 2(e) as dashed red lines, with the corresponding labels (c) and (d). The existence of contiguous blue areas extending from the nanotube to the metal Pd through the interface indicates that the electron from the nanotube can be ballistically transferred to the metal electrode. A more quantitative analysis of the same features is shown in Fig. 2(e), in which we plot the variation of electrostatic potential along the direction of four lines passing through C and Pd atoms. The colors of the curves in this figure correspond to the colors of the dashed lines shown in Fig. (c) and (d), which connect C atoms on the nanotube to their close Pd neighbors in the metal. The Fermi level is shifted to zero and denoted by a

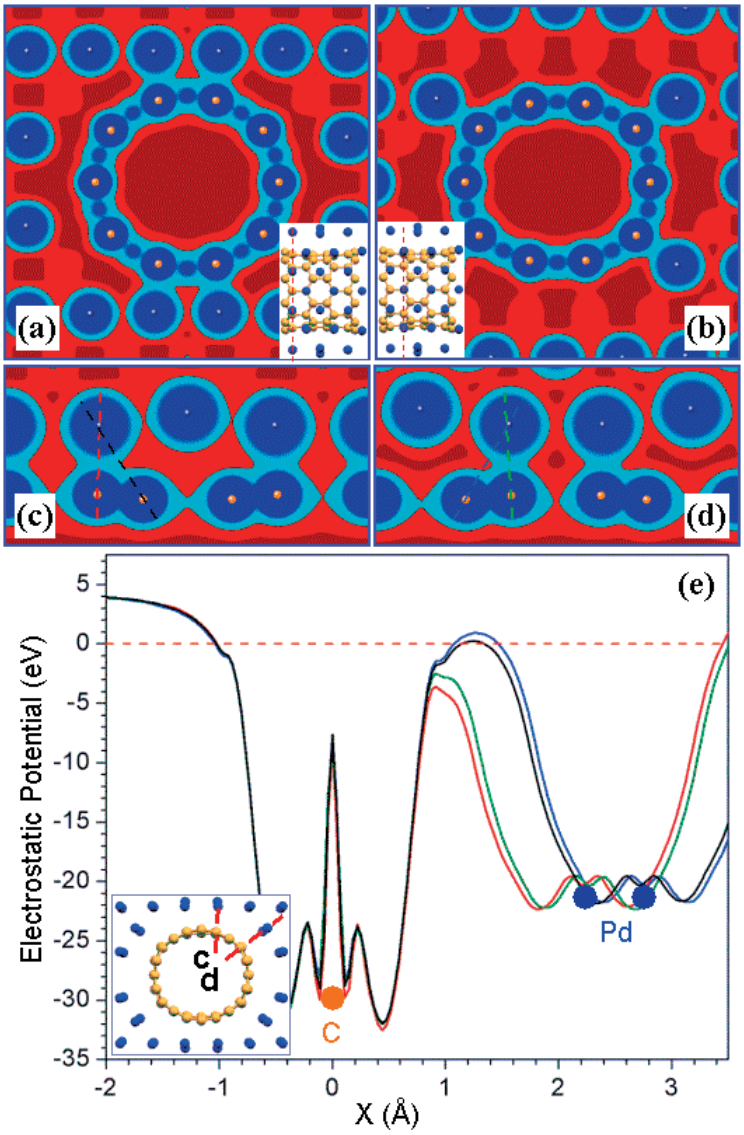

Fig. 2 (online colour at: www.pss-b.com) Calculated self-consistent electrostatic potential for the Pd-covered (10,0) nanotube: (a) and (b) contours of constant potential plotted in two cross-sections perpendicular to the nanotube axis, indicated by the red lines in the insets. In (c) and (d) the potential contours on two different cross-sections are shown, which are indicated by red lines in the inset of (e), with corresponding labels. In these plots, blue represents negative values and red positive values of the electrostatic potential, relative to the Fermi level. In (e), we show the electrostatic potential along four directions passing through C and Pd atoms near the contact region, and extending from the center of the nanotube ($x = -2$ Å) to well within the metal region ($x = +3$ Å); the colors of the curves correspond to the colors of the dashed lines indicating those directions in panels (c) and (d); the red dashed line indicates the Fermi level. In all panels C atoms are shown in orange and Pd atoms in blue; the positions of C atoms are set to zero in (e).

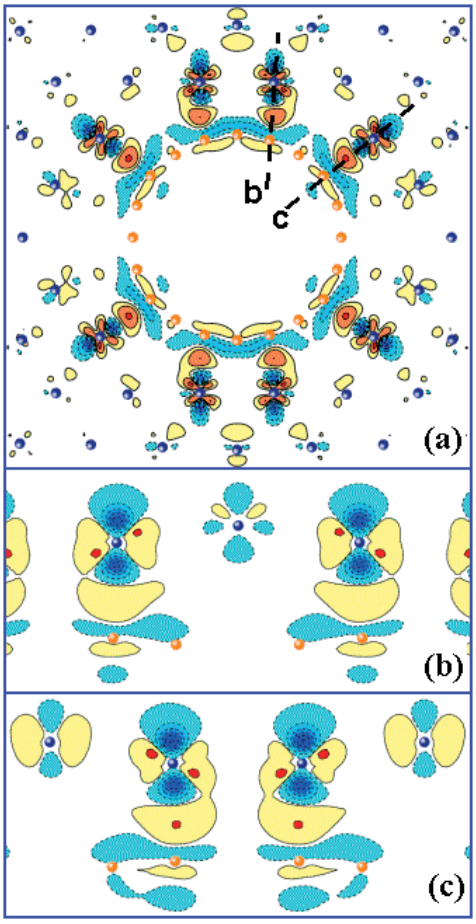

Fig. 3 (online colour at: www.pss-b.com) Charge density difference plots for the Pd-covered (10,0) nanotube: (a) integrated along the direction of the nanotube axis; (b) and (c): on the two cross sections indicated in (a) as black dashed lines. Yellow indicates accumulation of electronic charge density and blue depletion of electronic charge density. The positions of C and Pd atoms are denoted by symbols as in Fig. 2.

red dotted line. The line scans extend from the center of the tube ($x = -2$ Å) to well within the metal ($x = +3$ Å). As is clearly seen from this plot, the electrostatic potential is always lower than the Fermi level, by about ~3 eV at its highest value, along several paths from a C atom to a close neighbor Pd atom (the red and green line scans). Therefore, we conclude that there exist paths for electron transport from the nanotube to the metal region that do not involve any electrostatic barrier, which is consistent with previous calculations on (8,0) SWCNT adsorbed on Pd surfaces [15].

We next perform an analysis of charge transfer between the (10,0) SWCNT and the metal Pd electrode. Figure 3 shows the difference between the total electron density of the combined Pd/(10,0) SWCNT system and the sum of the total electron density of the isolated nanotube and pure metal Pd, the latter two having exactly the same structure when considered separately as the structure they have in the combined system. In Fig. 3(a), the charge density difference, integrated in the direction parallel to the nanotube axis, is plotted on the plane perpendicular to the nanotube axis. The blue regions represent depletion of electrons while the yellow regions represent accumulation of electrons in the combined system relative to the two isolated components. In Fig. 3(b) and (c) we show the same quantity on the two cross sections shown also in Fig. 2(c) and (d). This set of results presents clear evidence that electrons leave from both components of the system near the interface and accumulate in the interface region.

Figure 4 illustrates the evolution of the electronic states from the free to the metal-covered (10,0) nanotube. We plot the density of states (DOS) for the free standing (10,0) SWCNT (Fig. 4(a)), the isolated deformed nanotube in the structure it assumes when in contact with Pd electrode (the "deformed

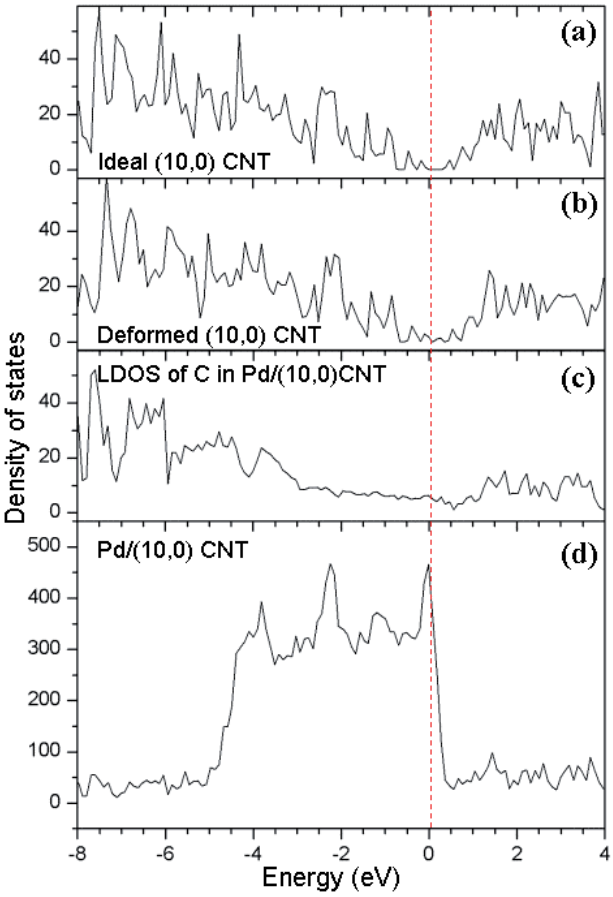

Fig. 4 (online colour at: www.pss-b.com) (a) DOS of a free standing (10,0) CNT; (b) DOS of an isolated (10,0) CNT with the atomic structure of that embedded in Pd; (c) projected DOS on C for the combined Pd/CNT system; (d) DOS of the combined Pd/CNT system. The vertical dotted red line denotes the Fermi level of the Pd/CNT system.

(10,0) CNT", Fig. 4(b)), and the Pd/nanotube combined system (Fig. 4(d)). We align the energy levels of different calculations with the average potential at the atomic core of a C atom, denoted by the arrow in Fig. 1(a). We find that the band gap of the semiconducting (10,0) SWCNT vanishes due to the deformation of the nanotube. Moreover, in the Pd/CNT system, the site-projected DOS on the C atoms (Fig. 4(c)) reveals that the interface states increase the DOS around the Fermi level in the combined system. The large density of states in the range within 5 eV below the Fermi level is due entirely to Pd d-states, which are nearly full. The position of the Fermi level is actually such that it requires some fraction of the Pd d-states to be partially filled, consistent with the partial depletion of electrons from the Pd side discussed in connection with the charge density difference.

In summary, we studied the electronic structure of semiconducting (10,0) SWCNTs fully covered by metal Pd electrode, in a geometry that is realistically close to experimental setup. We found that embedding the nanotube in a Pd metal electrode induces an obvious distortion relative to its ideal structure in vacuum. In addition, we found that there are no electrostatic potential barriers between the nanotube and the metal contact in the directions connecting C atoms to Pd close neighbors, along which the potential is always below the Fermi level. We also found that electrons are depleted from both sides of the interface and accumulate in the regions between the two components of the system. Finally, the deformation and the interface states lead to the vanishing of the (10,0) carbon nanotube band gap.

Acknowledgements We acknowledge helpful discussions with Phaedon Avouris. This work was sponsored by the Institute for the Theory of Advanced Materials in Information Technology (ITAMIT), University of Texas, Austin, which is funded by NSF grant No. DMR-0325218.

References

[1] S. Iijima, Nature **354**, 56 (1991).
[2] M. S. Dresselhaus, G. Dresselhaus, and Ph. Avouris, Carbon Nanotubes: Synthesis, Structure, Properties, and Applications (Springer Verlag, Berlin, 2001).
[3] S. Ciraci, S. Dag, T. Yildirim, O. Gülseren, and R. T. Senger, J. Phys.: Condens. Matter. **16**, R901 (2004).
[4] S. J. Tans, A. R. M. Verschueren, and C. Dekker, Nature **393**, 49 (1998).
[5] A. Bachtold, P. Hadley, T. Nakanishi, and C. Dekker, Science **294**, 1317 (2001).
[6] R. Martel, T. Schmidt, H. R. Shea, T. Hertel, and Ph. Avouris, Appl. Phys. Lett. **73**, 2447 (1998).
[7] R. Martel, V. Derycke, C. Lavoie, J. Appenzeller, K. K. Chan, J. Tersoff, and Ph. Avouris, Phys. Rev. Lett. **87**, 256805 (2001).
[8] A. Javey, J. Guo, Q. Wang, M. Lundstrom, and H. Dai, Nature **424**, 654 (2003).
[9] D. Mann, A. Javey, J. Kong, Q. Wang, and H. Dai, Nano Lett. **3**, 1541 (2003).
[10] S. Heinze, M. Radosavljević, J. Tersoff, and Ph. Avouris, Phys. Rev. B **68**, 235418 (2003).
[11] S. Heinze, J. Tersoff, R. Martel, V. Derycke, J. Appenzeller, and Ph. Avouris, Phys. Rev. Lett. **89**, 106801 (2002).
[12] F. Léonard and J. Tersoff, Phys. Rev. Lett. **84**, 4693 (2000).
[13] Z. Chen, J. Appenzeller, J. Knoch, Y.-M. Lin, and Ph. Avouris, Nano Lett. **5**, 1497 (2005).
[14] S. Dag, O. Gülseren, S. Ciraci, and T. Yildirim, Appl. Phys. Lett. **83**, 3180 (2003).
[15] B. Shan and K. Cho, Phys. Rev. B **70**, 233405 (2004).
[16] S. Okada and A. Oshiyama, Phys. Rev. Lett. **95**, 206804 (2005).
[17] J. P. Perdew, in: Electronic Structure of Solids '91, edited by P. Ziesche and H. Eschrig (Akademie Verlag, Berlin, 1991).
J. P. Perdew and Y. Wang, Phys. Rev. B **45**, 13244 (1992).
[18] G. Kresse and J. Furthmüller, Phys. Rev. B **54**, 11169 (1996).
[19] D. Vanderbilt, Phys. Rev. B **41**, 7892 (1990).
G. Kresse and J. Hafner, J. Phys.: Condens. Matter **6**, 8245 (1994).
[20] H. J. Monkhorst und J. D. Pack, Phys. Rev. B **13**, 5188 (1976).